INTEGRATED STRATEGY FOR HIGH EFFICIENCY AND LOW DEFECT WAFER PLANARIZATION PROCESSES

Lifei Zhang [1,2*], *Xinchun Lu* [1,2*]
[1] State Key Laboratory of Tribology in Advanced Equipment, Tsinghua University, Beijing, China
[2] Hwatsing Technology Co., Ltd., Tianjin, China
*Corresponding Author's Email: xclu@tsinghua.edu.cn

ABSTRACT

This work establishes a comprehensive integrated strategy for optimizing the performance of chemical mechanical polishing in semiconductor manufacturing at advanced technology nodes. These results demonstrate that the slurry injection position plays a critical role in determining flow distribution, which affects the material removal rate. By implementing a dynamic slurry sweep mode, the within-wafer non-uniformity could be enhanced by 53% and the slurry consumption could be reduced by 15%, concurrent with a relatively high material removal rate of ~4666 Å/min. Furthermore, a pre-cleaning process using cationic surfactants achieves 99.94% removal of particle residues, delivering an atomically smooth surface. Our proposed integrated strategy for high efficiency and low defect wafer planarization offers a holistic approach to addressing the challenges of advanced semiconductor manufacturing.

INTRODUCTION

Chemical mechanical polishing (CMP) technology is an indispensable approach to achieve wafer global planarization in integrated circuit manufacturing process. As the technology node advances to 3 nm and below, CMP faces dual challenges: optimizing the polishing process to achieve high material removal rate (MRR) and excellent within-wafer non-uniformity (WIWNU), achieving a nearly defect-free surface by post-CMP cleaning, especially the removal of slurry residues such as cerium dioxide (CeO_2) particles.

The distribution of slurry flow exerts a direct influence on mass transfer efficiency, abrasive uniformity, MRR, and WIWNU, collectively determining process performance. [1, 2]. Slurry distribution is closely related to its injection position, directly controlling the conveying and uniformity of the abrasive. Conventional optimization approaches primarily emphasize static parameters or the distribution of steady-state flow fields, often overlooking the evolution of dynamic flow behavior. This limitation restricts their effectiveness in informing cost control strategies for large-scale industrial production [3, 4]. Furthermore, for the CeO_2 nanoparticles that are difficult to remove, an innovative pre-cleaning process has been introduced [5, 6]. This not only avoids the damage to the device structure caused by traditional cleaning solutions with strong corrosiveness such as strong acids, strong alkalis, or oxidizing properties, but also effectively enhances the cleaning effect of chemical reactions on the particles. However, the mature cleaning process for 12-inch wafers and the mechanism of surfactants remain unclear, which restricts the further improvement of the actual process effect.

Therefore, in the face of the above challenges, our research reveals the basic mechanism of the influence of slurry injection position on flow dynamics and polishing uniformity. Based on this, a new slurry sweep mode was proposed to dynamically adjust the distribution, successfully balancing MRR, WIWNU and slurry consumption. Moreover, for the difficult removal of CeO_2 nanoparticles, an efficient pre-cleaning process using cationic surfactants was developed. The synergistic effect between the mechanical parameters and the chemical mechanisms was clarified to achieve an atomically smooth and defect-free surface.

EXPERIMENTAL

As shown in **Figure 1**, all CMP and pre-cleaning experiments were completed on a Universal-TS polisher, with the complete process flow of CMP, pre-cleaning, post-CMP cleaning, and drying. For the polishing stage, 12-inch wafers were polished for 30 seconds, employing a 7-zone pressure structure with all zones set to 2.25 psi to avoid pressure non-uniformity. In addition, computational fluid dynamics (CFD) software Fluent 2022 R2 was employed to establish a gas-liquid two-phase flow model and apply the sliding mesh technique for numerical simulation of the transient flow field under the slurry sweep mode, with boundary conditions strictly consistent with experimental parameters. The specific forms of these equations used are given below:

$$\frac{\partial \rho}{\partial t}+\nabla\cdot(\rho\vec{u})=0 \tag{1}$$

$$\rho\left(\frac{\partial u}{\partial t}(\vec{u})+\vec{u}\nabla\vec{u}\right)=-\nabla\rho+\left[\mu\left(\nabla\vec{u}+\vec{u}^{T}\right)\right]+\vec{F} \tag{2}$$

where ρ is the fluid density, t is time, $\vec{u}$ is the velocity vector, p is the fluid pressure, μ is the dynamic viscosity, and $\vec{F}$ is the external force vector per unit volume. The continuity equation governs the conservation of mass within a control volume over time, whereas the momentum equation describes the conservation and evolution of fluid momentum.

$$\frac{\partial}{\partial t}(\rho C)+\nabla\cdot(\rho\vec{u}C)=\rho D\nabla^2 C \quad (3)$$

where C is the slurry concentration, and D is the diffusion coefficient. This equation describes the transport of solute species within the slurry. All governing equations are solved numerically using the finite volume method following discretization.

The pre-cleaning process parameters, including pressure, head/platen speed, deionized water (DIW) flow rate, and cleaning time, were optimized through single-factor experiments, using the number of particles on the wafer surface as the evaluation metric. To assess the effect of surfactants, two each of nonionic (AEO-9, APG1214), anionic (DBSA, AES), and cationic (CAB, CTAB) types were selected to prepare 2000 ppm cleaning solutions at pH=10 for pre-cleaning experiments. The cleaning effectiveness was evaluated by macroscopic defect statistics using a wafer defect inspection system (Surfscan SP7) while the surface morphology and roughness were assessed using atomic force microscopy (AFM). The cleaning mechanism was investigated by XPS analysis of Ce^{3+}/Ce^{4+} and O 1s, complemented by AFM adhesion force measurements, zeta potential analysis of electrostatic interactions, and quantum chemical/molecular dynamics simulations (Gaussian 16W/Materials Studio) of surfactant adsorption.

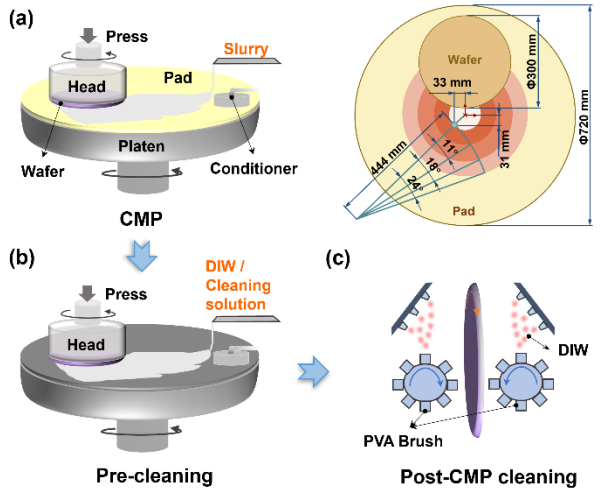

Figure 1: Process flow diagram.

RESULT AND ANALYSIS

CMP costdown by applying a slurry sweep mode

Figure 2 shows the simulation results of CFD under different slurry sweep modes. During the CMP process, the slurry is dispensed beneath the rotating wafer, where it facilitates material removal through synergistic chemical and mechanical actions. An aggregated slurry layer forms on the pad surface, and its spatial distribution critically determines the amount and location of slurry that enters the wafer–pad interface. The dispersion patterns of the slurry volume fraction are markedly influenced by the sweep trajectory. For a trajectory of 45–100 mm, the average slurry content across the pad remains relatively high, leading to an increased local volume fraction on the wafer surface. In contrast, extending the trajectory to 45–210 mm significantly reduces the variation in volume fraction across different regions of the wafer, resulting in a substantial improvement in uniformity. In addition, the slurry sweep trajectory also significantly affects the flow state of the slurry. According to the simulation results, a shorter sweep trajectory intensifies the shear effect from slurry flow on the wafer surface but elevates the risk of non-uniformity by forming localized high-shear regions. In contrast, a longer sweep trajectory mitigates average shear stress and facilitates a more homogeneous shear force distribution.

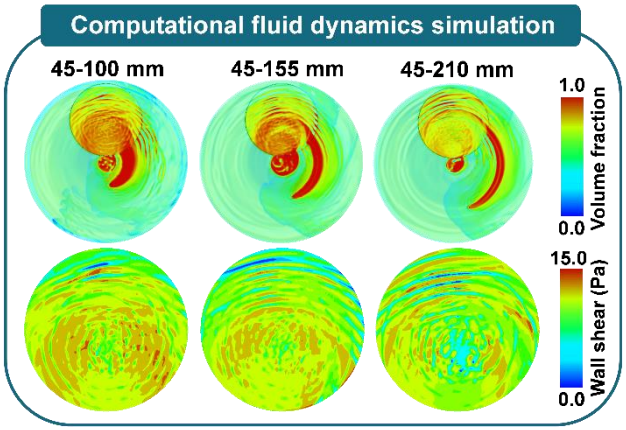

Figure 2: CFD simulation results.

Our previous study has indicated that the slurry demand varies across different locations on the wafer [7]. To mitigate this non-uniformity issue, the slurry injection position must be capable of dynamic adjustment. Accordingly, a series of slurry sweep recipes were developed to examine their influence on process performance, as illustrated in **Figure 3**. As the slurry sweep end position moves closer to the pad edge, the MRR at the wafer center increases, leading to a corresponding rise in the overall MRR. This implies that the wafer center has a relatively lower demand for slurry, therefore, the dwell time of the slurry sweep in this region should be reduced. A comparison of the MRR profiles from Sweep 2 and Sweep 3 reveals that the WIWNU was improved following the adjustment of the sweep dwell time ratio. With a sweep trajectory of 45–210 mm, a dwell time ratio of 3:1:1, and a flow rate of 170 mL, the MRR measures approximately 4666 Å/min, closely matching the baseline value. Furthermore, compared to the fixed injection method, this optimized sweep configuration achieves a 15% reduction in slurry consumption while improving WIWNU by 53%. Surface roughness of the wafers was

measured by AFM under static (without sweep) and dynamic (with sweep) slurry injection conditions. The results demonstrated that the slurry sweep mode effectively enhances wafer surface quality compared to a fixed injection position.

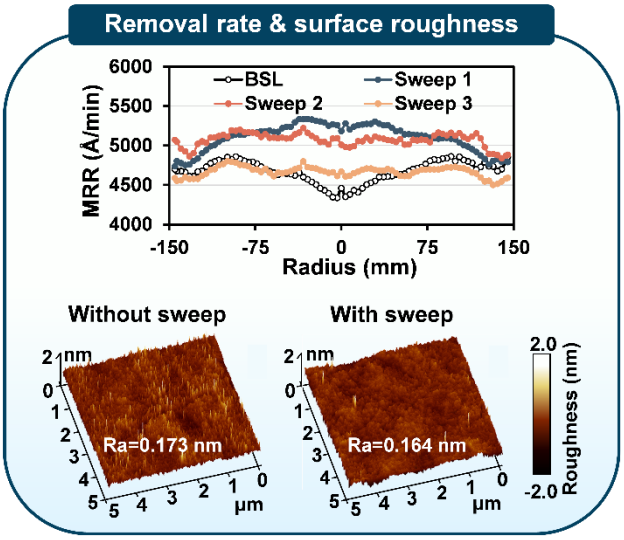

Figure 3: CMP process experimental results.

Tribochemical synergistic cleaning strategy for the pre-cleaning process

Figure 4a systematically illustrates the influence of various pre-cleaning process parameters on particle removal efficiency. Wafer defect scan results indicate that the introduction of the pre-cleaning step leads to a significant reduction in surface-adhered particles. Pressure from the polishing head increases mechanical shear, thereby detaching particles from the substrate by overcoming the adhesive forces. The rotational speed of the polishing head/platen is a pivotal factor on which the cleaning outcome critically depends. Optimal particle removal is achieved at 107/113 RPM, indicating that this speed facilitates a favorable balance among hydrodynamic forces, shear stress, and the contact state between the polishing pad and the wafer. When DIW is used as the sole cleaning medium, variations in flow rate show no significant impact on the removal of residual CeO_2 particles on the wafer surface. Furthermore, the count of residual particles decreases rapidly with increasing cleaning time and then gradually plateaus. Considering throughput, the processing time of 20 s is adequate to satisfy cleaning performance requirements. The optimal process parameters under the experimental conditions are determined as follows: pressure of 2 psi, head/platen speed of 107/113 RPM, DIW flow rate of 300 ml/min, and processing time of 20 s. A comparison of defect maps with and without the pre-cleaning step (**Figure 4b**) clearly demonstrates that the pre-cleaning process significantly enhances wafer surface quality and morphology uniformity.

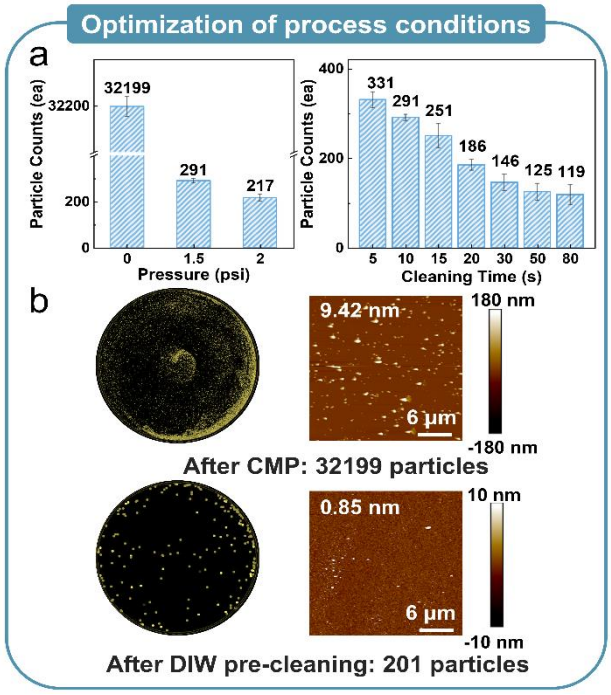

Figure 4: Correlation between pre-cleaning process parameters and ceria particle removal efficiency.

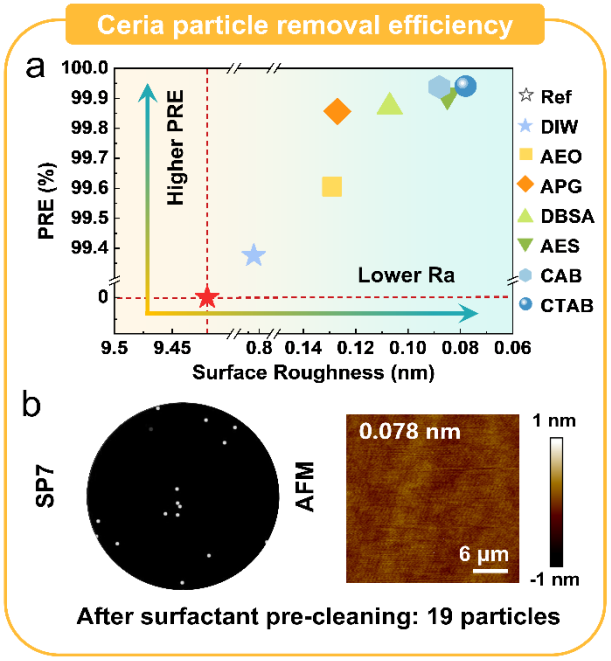

Figure 5: Evaluation of synergistic effects between different surfactant types and process.

To further elucidate the function of chemicals in particle removal, DIW was replaced with surfactants as the cleaning medium. The cleaning performance of non-ionic (AEO and APG), anionic (DBSA and AES), and cationic

(CAB and CTAB) surfactants was systematically compared, as shown in **Figure 5**. The synergy between surfactants and process conditions enhances the removal of ceria particles. The ranking of cleaning efficiency and surface quality are as follows: cationic > anionic > non-ionic surfactants. Upon treatment with CTAB, the wafer yields a residual particle count of 19 and maintains a surface roughness of just 0.078 nm, meeting the stringent requirements of high-end processes for surface quality.

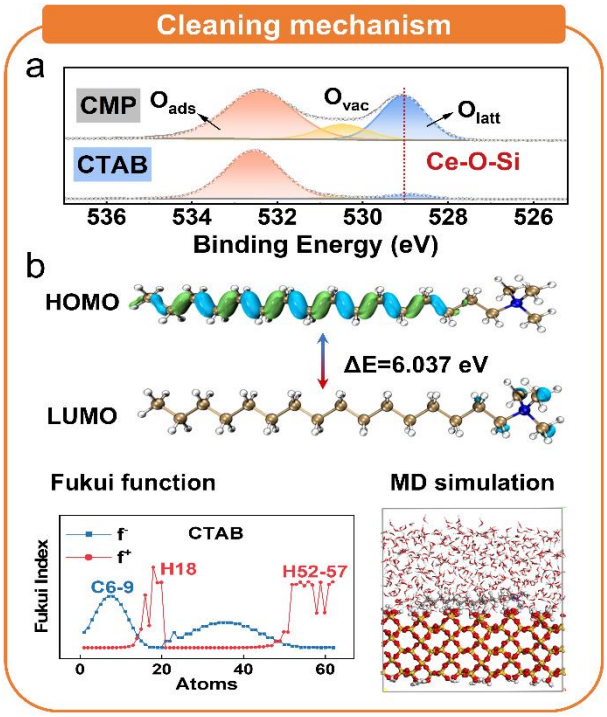

Figure 6: Analysis of the mechanism for CTAB in removing ceria particles.

XPS analysis was employed to examine SiO_2 surfaces treated under different conditions (**Figure 6a**), aiming to gain deeper insight into the bonding behavior during the cleaning process. The O1s spectra can be fitted with three characteristic peaks, corresponding to lattice oxygen (O_{latt}) at approximately 529.0 eV, oxygen vacancies (O_{vac}) at ~530.6 eV, and adsorbed oxygen (O_{ads}) at ~532.5 eV. The lattice oxygen corresponds to the Ce–O bond within CeO_2 and is intimately associated with the Ce–O–Si bond. This spectral feature near 529 eV has been cited as evidence of Ce–O–Si bond formation in the literature (e.g., Sahir and Munusamy). Accordingly, we monitored variations in the relative area of the O_{latt} peak. After cleaning with the cationic surfactant CTAB, the proportion of O_{latt} peak decreased significantly. **Figure 6b** illustrates the calculated quantum chemical parameters of CTAB in a liquid environment, including the highest occupied molecular orbital (HOMO), the lowest unoccupied molecular orbital (LUMO), the energy gap (ΔE) and Fukui function. In CTAB, the HOMO is mainly localized on the hydrophobic hexadecyl chain, whereas the LUMO resides on the hydrophilic quaternary ammonium group. This spatial distribution allows the LUMO to serve as an effective electron-acceptor site, thereby facilitating local electron transfer at the solid–liquid interface and potentially promoting the oxidation of Ce^{3+}. Combined with the mechanical friction provided by the pre-cleaning process, CTAB synergistically disrupts the Ce-O-Si bonds, enabling efficient particle removal and demonstrating good process compatibility and potential for industrial application.

CONCLUSIONS

This work establishes a comprehensive strategy for optimizing CMP performance. The results show that the slurry injection position critically determines flow distribution, directly influencing MRR. A dynamic sweep trajectory was subsequently developed, successfully enhancing WIWNU and reducing slurry consumption by 15% without sacrificing MRR. Furthermore, a pre-cleaning process utilizing cationic surfactant CTAB was engineered to achieve a CeO_2 cleaning efficiency of 99.94% and an atomic-level surface smoothness via a synergistic mechanism. These findings validated by CFD simulation and molecular calculation, provide a unified solution for high-performance, cost-effective, and defect-minimized CMP, crucial for advanced semiconductor manufacturing.

ACKNOWLEDGEMENTS

The authors gratefully acknowledge the Tsinghua University Initiative Scientific Research Program and Hwatsing Technology Co., Ltd..

REFERENCES

[1] M. Bahr, Y. Sampurno, R. Han, A. Philipossian. Micromachines-Basel, vol. 8, 2017, pp. 170.
[2] S. Oh, J. Seok. Wear, vol. 266, 2009, pp. 839-849.
[3] J. Sorooshian, D. DeNardis, L. Charns, Z. Li, F. Shadman, D. Boning, D. Hetherington, A. Philipossian, J. Electrochem. Soc., vol. 151, 2004, pp. 85.
[4] H. Lee, D. A. Dornfeld, H. Jeong, Int. J. Pr. Eng. Mangt., vol. 1, 2014, pp. 11-15.
[5] P. Liu, Y. Nam, S. Jeon, C. Kim, E. Kim, S. Choi, S. Lee, S.-H. Park, S. Hong, T. Kim, Colloids Surf. A Physicochem. Eng. Asp., vol. 671, 2023, pp. 131558.
[6] J. Kim, S. Hong, E. Kim, J. Lee, D. Kwak, Y. Wada, H. Hiyama, S. Hamada, T. Kim, ECS J. Solid State SCi., vol. 9, 2020, pp. 084003.
[7] L. Zhang, N. Zhao, H. Ci, D. Zhao, X. Lu, Friction, 2025, pp. 9441185.